THE JOURNAL OF BIOLOGICAL CHEMISTRY VOL. 291, NO. 36, pp. 18778–18790, September 2, 2016

The San1 Ubiquitin Ligase Functions Preferentially with Ubiquitin-conjugating Enzyme Ubc1 during Protein Quality Control*

Received for publication, May 10, 2016, and in revised form, July 7, 2016 Published, JBC Papers in Press, July 12, 2016, DOI 10.1074/jbc.M116.737619

Rebeca Ibarra[‡], **Daniella Sandoval**[‡], **Eric K. Fredrickson**[§], **Richard G. Gardner**[§], **and Gary Kleiger**[‡1]

From the [‡]*Department of Chemistry and Biochemistry, University of Nevada, Las Vegas, Nevada 89154 and the* [§]*Department of Pharmacology, University of Washington, Seattle, Washington 98195*

Protein quality control (PQC) is a critical process wherein misfolded or damaged proteins are cleared from the cell to maintain protein homeostasis. In eukaryotic cells, the removal of misfolded proteins is primarily accomplished by the ubiquitin-proteasome system. In the ubiquitin-proteasome system, ubiquitin-conjugating enzymes and ubiquitin ligases append polyubiquitin chains onto misfolded protein substrates signaling for their degradation. The kinetics of protein ubiquitylation are paramount as a balance must be achieved between the rapid removal of misfolded proteins *versus* providing sufficient time for protein chaperones to attempt refolding. To uncover the molecular basis for how PQC substrate ubiquitylation rates are controlled, the reaction catalyzed by nuclear ubiquitin ligase San1 was reconstituted *in vitro*. Our results demonstrate that San1 can function with two ubiquitin-conjugating enzymes, Cdc34 and Ubc1. Although Cdc34 and Ubc1 are both sufficient for promoting San1 activity, San1 functions preferentially with Ubc1, including when both Ubc1 and Cdc34 are present. Notably, a homogeneous peptide that mimics a misfolded PQC substrate was developed and enabled quantification of the kinetics of San1-catalyzed ubiquitylation reactions. We discuss how these results may have broad implications for the regulation of PQC-mediated protein degradation.

For cells to maintain proteostasis, a delicate balance must exist between protein biogenesis and degradation. The ubiquitin-proteasome system is a network of proteins and enzymes responsible for 70–80% of intracellular protein degradation in eukaryotic cells (1). The signal for protein degradation is the assembly of a polyubiquitin chain onto protein substrate.

Ubiquitylation occurs through the sequential action of three enzymes: E1[2] (ubiquitin-activating enzyme), E2 (ubiquitin-conjugating enzyme), and E3 (ubiquitin ligase) (2–5). E1 activates ubiquitin, a highly conserved 76-amino acid protein forming a thioester bond between the C-terminal carboxyl group on ubiquitin and a cysteine residue located within the E1 active site. Next, ubiquitin is transferred from E1 to E2. The E2∼ubiquitin (∼ is used to denote a thioester bond) is then recruited by an E3, which brings the E2∼ubiquitin and protein substrate into proximity. E3s may also participate in ubiquitylation by stimulating the ubiquitin transfer activity of E2s (6–11). In most cases ubiquitin is transferred from E2∼ubiquitin to the protein substrate, forming an isopeptide bond between the ubiquitin C terminus and a lysine residue on the substrate. The dissociation of E2s from E3 and the binding of fresh E2∼ubiquitin complexes enables the formation of a polyubiquitin chain on the substrate. Typically, a chain of at least four ubiquitins is required for a substrate to be recognized by the 26S proteasome for degradation (12, 13); however, the modification of several lysine residues with a single ubiquitin on some substrates may also be sufficient (14, 15).

PQC is a collection of critical pathways within the ubiquitin-proteasome system that are responsible for removing misfolded proteins from the cell (16). PQC systems are prevalent throughout the cell and can be found at important multisubunit complexes such as the ribosome (17–20) and in the cytoplasm (21–25) and organelles such as the endoplasmic reticulum (26, 27), mitochondria (28), and nucleus (29). Not surprisingly, the breakdown of normal PQC function may lead to several human diseases. For instance, lesions formed in patients with neurodegenerative diseases including Huntington, Alzheimer, and Parkinson contain a conglomeration of aggregated proteins including ubiquitin-proteasome system enzymes as well as numerous polyubiquitylated proteins that have evaded degradation (30, 31). Furthermore, mutations in several key enzymes that promote mitophagy through ubiquitylation-specific mechanisms have been found in patients with Parkinson disease (32–34). Finally, inclusions associated with Huntington disease are localized to the nucleus, suggesting a breakdown of nuclear PQC processes in those patients (35, 36).

Nuclear PQC in the budding yeast *Saccharomyces cerevisiae* is controlled by the San1 ubiquitin ligase (29, 37). San1 contains highly disordered regions that identify misfolded substrates by binding to exposed hydrophobic stretches on the substrate (38–43). Genetic results have suggested that San1 recruits the E2s Cdc34 and Ubc1 to form polyubiquitin chains on misfolded proteins (29). Interestingly, previous work has shown that many

* This work was supported, in whole or in part, by National Institutes of Health Grant P20 GM103440 and R15 GM117555-01 (NIGMS; to G. K. and R. I.). The authors declare that they have no conflicts of interest with the contents of this article. The content is solely the responsibility of the authors and does not necessarily represent the official views of the National Institutes of Health.

[1] To whom correspondence should be addressed: Dept. of Chemistry and Biochemistry, University of Nevada, Las Vegas, 4505 S. Maryland Pkwy., Las Vegas, Nevada 89154-4003. Tel.: 702-895-3585; Fax: 702-895-4072; E-mail: gary.kleiger@unlv.edu.

[2] The abbreviations used are: E1, ubiquitin-activating enzyme; E2, ubiquitin-conjugating enzyme; E3, ubiquitin ligase; PQC, protein quality control; APC, anaphase promoting complex; SCF, Skp1-cullin-Fbox; KR San1, no lysine San1.

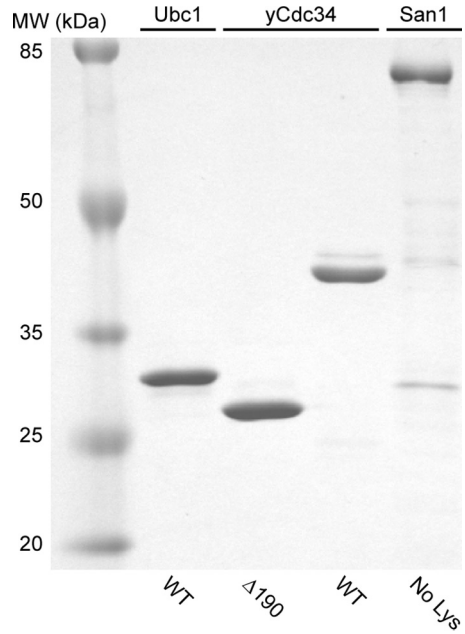

FIGURE 1. **The final purities of WT Cdc34, Δ190 Cdc34 lacking the acidic tail, WT Ubc1, and full-length San1.** Approximately 1 μg of protein was loaded onto a SDS-PAGE gel that, after electrophoresis, was stained with Coomassie Blue. The final purity for KR (No Lys) San1 is shown and is similar to the purities of all San1 constructs.

E3s ubiquitylate their protein substrates with at least two distinct members of the E2 family (44–50). In these examples, an E2 initiates polyubiquitin chain formation by transferring the first ubiquitin to the E3-bound substrate, whereas a different E2 is responsible for chain elongation. Thus, it is possible that San1 may also function synergistically with both Cdc34 and Ubc1 during nuclear PQC substrate ubiquitylation. However, it is also possible that Cdc34 and Ubc1 may function independently with San1.

To distinguish between these 2 hypotheses, an *in vitro* PQC ubiquitylation system was reconstituted containing E1, ubiquitin, San1, a PQC substrate, and either Cdc34 or Ubc1 alone or in combination. Our results show robust E3-dependent ubiquitylation of substrate in the presence of either Ubc1 or Cdc34; however, Ubc1 consistently shows greater activity with San1 than does Cdc34. Furthermore, to the best of our knowledge, we have developed the first homogeneous peptide substrate for PQC, enabling the use of quantitative enzyme kinetics to characterize the San1 ubiquitylation reaction. The results from these experiments suggest that San1 prefers to function with Ubc1, even in the presence of Cdc34.

Results

To uncover whether Cdc34 and Ubc1 may function synergistically with San1, an *in vitro* ubiquitylation reaction was reconstituted that detected San1 autoubiquitylation. Full-length San1 protein was expressed and purified from bacterial cells (Fig. 1). Because a single lysine San1 would allow for the specific monitoring of polyubiquitin chain formation without the potentially confounding effects of multi-monoubiquitylation, all naturally occurring San1 lysine residues were mutated to arginine, and a single lysine was introduced at Asn-13 because previous experiments in yeast demonstrated that N13K San1 was both autoubiquitylated and capable of binding to misfolded proteins (38).

Radiolabeled N13K San1 was rapidly ubiquitylated in the presence of E1, ubiquitin, and WT yeast Cdc34 (Fig. 2*A*). The formation of extensive polyubiquitin chains on N13K San1 was evident as early as 15 s. The fraction of San1 proteins that had been modified by one or more ubiquitins was linear during the time course, enabling the determination of the rate of ubiquitylation (some 14% of San1 was modified per minute; Fig. 2*B*). Furthermore, the location of the single lysine at the N terminus of San1 was not important for promoting San1 autoubiquitylation, as a San1 protein containing a single lysine at the C terminus, N444K San1, was autoubiquitylated with similar kinetics as N13K San1 (Fig. 2, *C* and *D*).

Most E3s contain a conserved RING domain that recruits E2∼ubiquitin (2). N13K San1 that contained an additional mutation known to disrupt RING-E2 interactions (10) (N13K/R280A San1) was produced and was incapable of autoubiquitylation (Fig. 2*E*), demonstrating that San1 activity was dependent on the interaction between Cdc34∼ubiquitin and the San1 RING domain.

San1 autoubiquitylation was next assayed in the presence of WT Ubc1. Polyubiquitin chain formation on N13K San1 was substantially more rapid than in the presence of Cdc34, and the polyubiquitin chains were longer as well (Fig. 3*A*). Although the amount of N13K San1 autoubiquitylated product quickly diverged from linearity during the time-course (Fig. 3*B*), the data fit well to a single phase exponential function, allowing for the estimation of the initial rate of San1 modification (see "Experimental Procedures") and comparison to the rate of San1 autoubiquitylation with Cdc34. Impressively, the rate of San1 ubiquitylation was nearly eight times greater in the presence of Ubc1 than with Cdc34. San1 autoubiquitylation was greatly reduced in the presence of N13K/R280A San1, although some product formation was evident toward the end of the time course (Fig. 3*C*), hinting that Ubc1 may have greater affinity for San1 and/or greater catalytic activity in the presence of San1 as compared with Cdc34. Finally, similar to reactions containing Cdc34, N444K San1 was also rapidly autoubiquitylated in the presence of Ubc1 (Fig. 3, *D* and *E*).

E2 activity is often stimulated in the presence of E3 through highly specific interactions at the E2∼ubiquitin-E3 interface (6–11). However, E2 activation only occurs for selective E2-E3 pairs, and E2 stimulation by an E3 *in vitro* is, therefore, evidence of a functional interaction. To explore this possibility for San1 and either Cdc34 or Ubc1, we used a previously described assay (51) that measures E2 activity in either the absence or presence of San1. Briefly, E2 is first thioesterified to ^{32}P-labeled ubiquitin with E1, and the reaction is then initiated by adding unlabeled ubiquitin. Chain formation between unlabeled and labeled ubiquitin results in the formation of a diubiquitin product. WT Cdc34 activity was first measured in the absence of San1 (Fig. 4, *A* and *G*, and Table 1). The same reaction was then repeated in the presence of KR San1 that contains no lysine residues and, therefore, does not get autoubiquitylated (note that KR San1 can replace endogenous San1 *in vivo*; Ref. 38). The addition of KR San1 resulted in a 2-fold increase in Cdc34 activity (Fig. 4, *B* and *G*, and Table 1). This modest increase in Cdc34 activity was

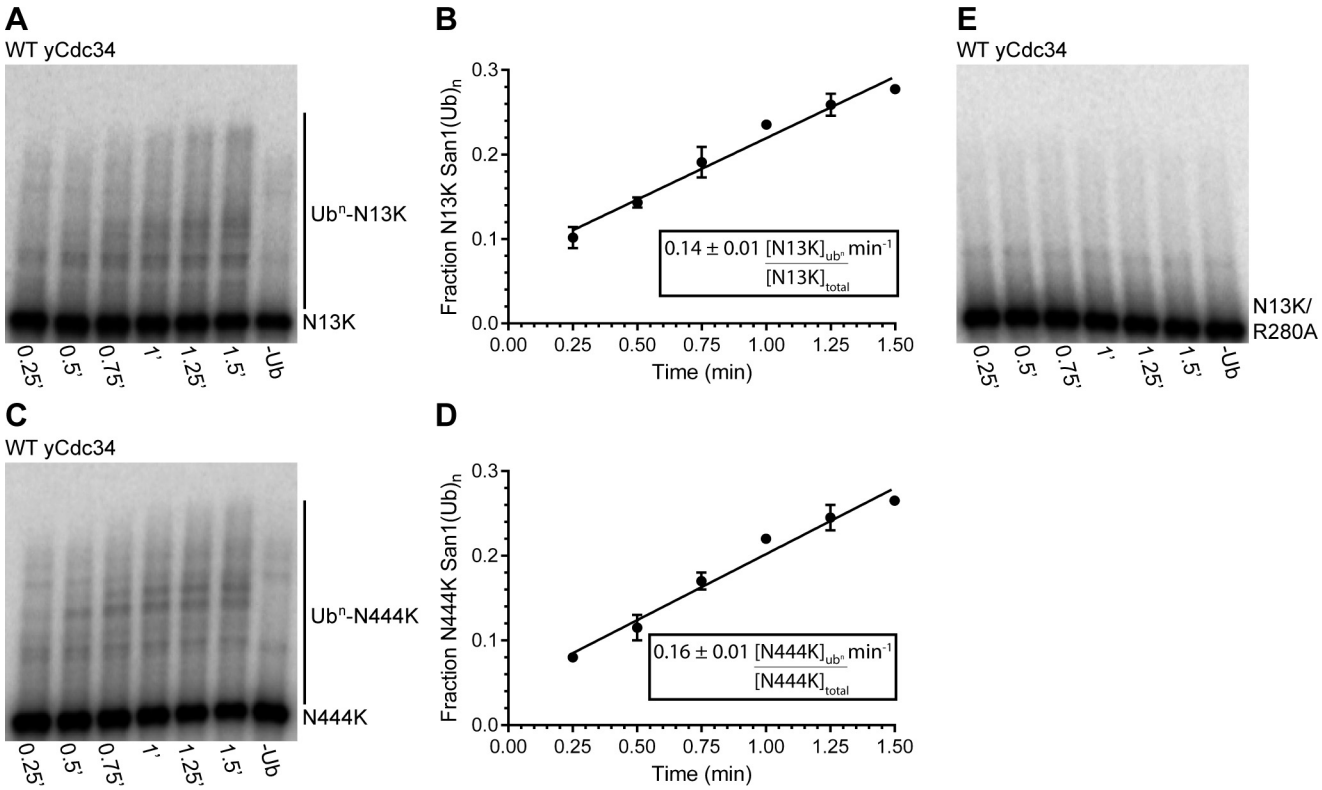

FIGURE 2. **Single lysine San1 is rapidly autoubiquitylated in the presence of WT Cdc34.** *A*, time-course showing autoubiquitylation of radiolabeled N13K San1 in the presence of WT Cdc34, E1, and ubiquitin. Product is defined as any San1 protein that has been modified by one or more ubiquitins. *B*, quantitation of the fraction of N13K San1 that was converted to ubiquitylated product. Notice that the fraction of San1 product was linear with respect with time. *Error bars* represent the S.E. of measurements from duplicate data points. *C*, same as in *A* but with N444K San1. *D*, same as in *B* but with N444K San1. *E*, same as in *A* but with N13K/R280A San1.

dependent on Cdc34 binding to the San1 RING domain, as N13K/R280A San1 did not activate Cdc34 (Fig. 4, *C* and *G*, and Table 1).

Although KR San1 increased Cdc34 activity by 2-fold, this result was unimpressive, as Cdc34 activity was greatly stimulated in the presence of the human SCF subunits Cul1-Rbx1 (Fig. 4, *D* and *H*, and Table 1). Indeed, the stimulation of WT Cdc34 activity by Cul1-Rbx1 was comparable to the stimulation of human Cdc34 (Ube2R1/2) activity by Cul1-Rbx1 (Fig. 4, *E*, *F*, and *H*, and Table 1). Thus, San1 activation of yeast Cdc34 was modest when compared with Cdc34 activation by Cul1-Rbx1.

The activity of Ubc1 was next measured using the diubiquitin synthesis assay in both the presence and absence of KR San1. Interestingly, E3-independent Ubc1 activity was 10 times slower in comparison with yeast Cdc34 (Fig. 5, *A* and *E*, and Table 1). However, the presence of KR San1 stimulated Ubc1 activity by ~38-fold and in a RING-dependent manner (Fig. 5, *B*, *C*, and *E*, and Table 1). Furthermore, the stimulation of Ubc1 by San1 was specific, as the presence of Cul1-Rbx1 had no effect on Ubc1 activity (Fig. 5, *D* and *E*, and Table 1). Taken together, these results demonstrate than San1 is capable of activating both yeast Cdc34 and Ubc1, although Ubc1 stimulation by San1 is far more impressive.

The results presented thus far suggest that although both WT Cdc34 and Ubc1 can function *in vitro* with San1, Ubc1 has greater activity and is also stimulated to a far greater extent in the presence of San1. However, the mechanism of San1 autoubiquitylation may differ substantially in comparison with a reaction involving a San1-bound PQC substrate. To address this, a *bona fide* PQC substrate that would enable quantitative enzyme kinetics was developed.

It had previously been shown that introducing a small, hydrophobic patch in the San1 amino acid sequence resulted in increased turnover of San1 protein in yeast (38). In those experiments, the RING domain in San1 had been mutated to eliminate autoubiquitylation. Finally, the mutant San1 protein was rapidly degraded in cells containing endogenous WT San1 but not in cells where the San1 gene had been deleted. Thus, the hydrophobic San1 protein mimics a PQC substrate that is recognized by endogenous San1. We reasoned that a synthetic peptide containing the hydrophobic patch and a single nearby lysine residue at the C terminus may function as a minimal San1 substrate *in vitro*. To help increase the peptide's solubility in aqueous buffer, 13 residues immediately N-terminal to the hydrophobic patch in San1 were also included as many of the residues are hydrophilic.

San1 peptide ubiquitylation reactions were first assembled in the presence of KR San1 and WT Cdc34. Polyubiquitin chains were rapidly assembled onto the San1 peptide but not in reactions lacking San1 (Fig. 6*A*). Furthermore, the peptide was not ubiquitylated in the presence of N13K/R280A San1, indicating that an intact RING domain was required to recruit Cdc34 (Fig. 6*A*). Because it is well known that Cdc34 generates Lys-48-specific polyubiquitin chains on SCF-bound substrates (52), the chain linkage specificity of the chains on the San1 peptide was also assessed. Indeed, San1 peptide ubiquitylation was similar

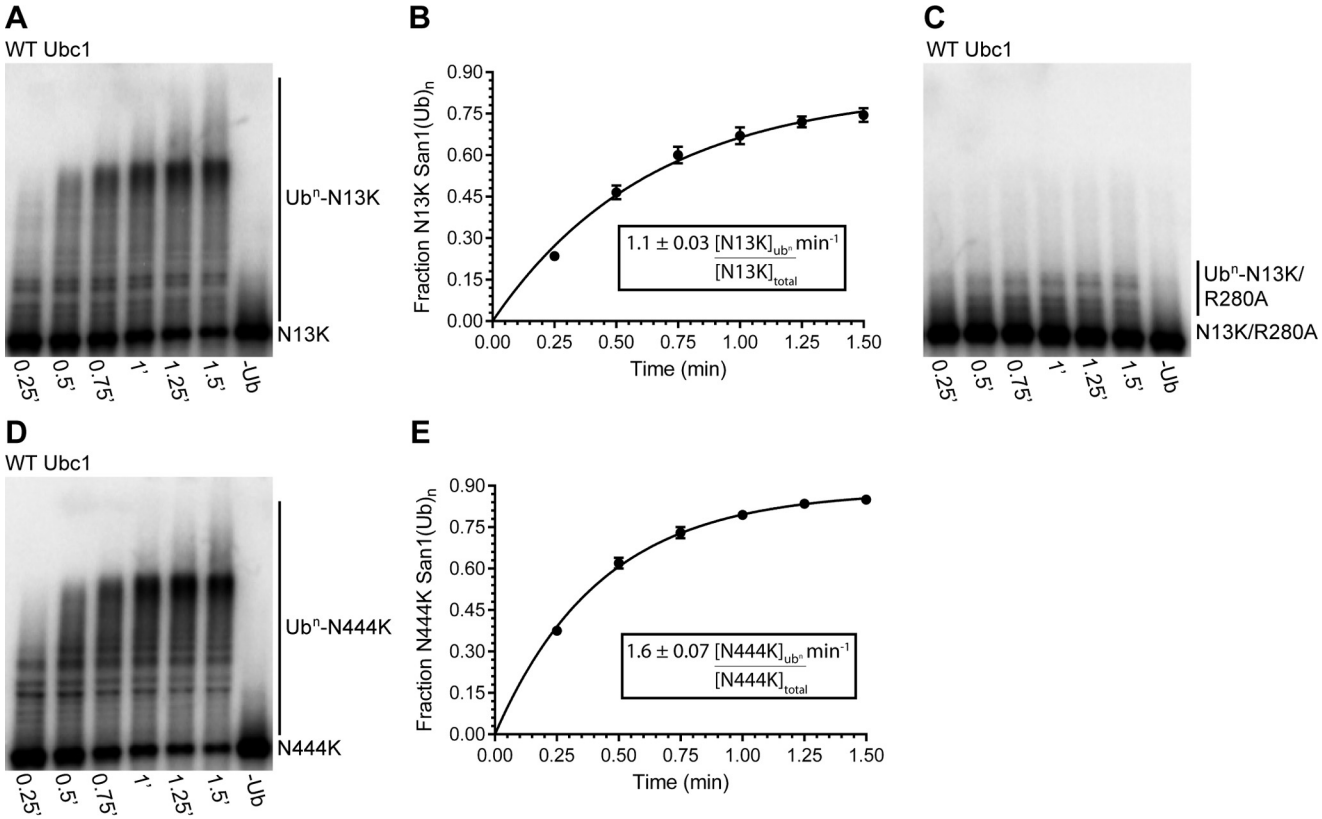

FIGURE 3. **Single lysine San1 is autoubiquitylated more rapidly in the presence of WT Ubc1 than with Cdc34.** *A*, time-course showing autoubiquitylation of radiolabeled N13K San1 in the presence of WT Ubc1, E1, and ubiquitin. *B*, quantitation of the fraction of N13K San1 that had been modified by one or more ubiquitins. Notice that product formation strays from linearity early in the time-course due to rapid conversion of San1 into product. *Error bars* represent the S.E. of measurements from duplicate data points. *C*, same as in *A* but with N13K/R280A San1. *D*, same as in *A* but with N444K San1. *E*, same as in *B* but with N444K San1.

in reactions comparing either WT ubiquitin or a ubiquitin mutant in which all lysine residues except Lys-48 had been mutated to arginine (Fig. 6*B*). San1 peptide ubiquitylation reactions were next assembled in the presence of KR San1 and WT Ubc1. Similar to Cdc34, polyubiquitin chains were rapidly assembled onto the San1 peptide in the presence of Ubc1 in a Lys-48-dependent manner (Fig. 6*B*).

One caveat regarding *in vitro* reconstituted ubiquitylation reactions is that non-physiological E2-E3 pairs are often active in the presence of very high concentrations of E2, whereas physiological E2-E3 pairs will typically interact with high affinity. The *in vitro* ubiquitylation system with San1 peptide enabled estimation of the K_m of either Cdc34 or Ubc1 for San1. Note that the K_m of an E2 for E3 has a long-standing history as a proxy of E2-E3 affinity, including in studies involving Cdc34 and ubiquitin ligase SCF, Ubc1, and the anaphase promoting complex (APC) ubiquitin ligase as well as numerous other E2-E3 pairs (46, 51, 53).

The K_m of either Cdc34 or Ubc1 for San1 was estimated by measuring the rate of San1 peptide ubiquitylation in the presence of varying concentrations of E2. The K_m of WT yeast Cdc34 was 1.7 μM for San1 (Fig. 7*A*). This was unexpected considering that the K_m of WT Cdc34 for yeast SCF is ~0.2 μM, demonstrating that Cdc34 has substantially weaker affinity for San1 in comparison to SCF. On the other hand, the K_m of WT Ubc1 was 0.09 μM for San1 (Fig. 7*B*), nearly 19-fold lower than in comparison with Cdc34. Interestingly, this value is also substantially lower than the K_m of Ubc1 for the APC (which is well known to function with Ubc1 *in vivo*) (46), indicating that Ubc1 has greater affinity for San1 than for the APC.

Cdc34 contains an atypical C-terminal extension with several highly conserved acidic residues. This domain (termed the acidic tail) has been shown to be a critical determinant in the high affinity binding of Cdc34 to SCF (53). To ascertain whether the Cdc34 acidic tail has a role in promoting Cdc34 binding to San1, a Cdc34 tail deletion mutant, Δ190 Cdc34, was purified, and its K_m for San1 was estimated. The K_m of Δ190 Cdc34 for San1 was 2.2 μM (Fig. 7*C*), comparable with the K_m of WT Cdc34 for San1. Thus, the Cdc34 acidic tail does not affect the binding of yeast Cdc34 to San1.

To determine if Cdc34 and Ubc1 function synergistically, San1 peptide ubiquitylation was initiated in the presence of either Cdc34 or Ubc1 alone or together (Fig. 8*A*), and the fraction of San1 peptide products containing one or more ubiquitins was quantified (Fig. 8*B*). Although reactions containing WT Cdc34 resulted in polyubiquitin chain formation on the San1 peptide as early as 1.5 min into the time-course, product formation with Ubc1 was even more robust and apparent as early as 45 s. Additionally, the formation of long polyubiquitin chains onto substrate (*visualized as smears toward the top of the gel*) was favored in reactions containing Ubc1 alone in comparison with those containing Cdc34 alone.

The presence of equal concentrations of both Ubc1 and Cdc34 in the presence of KR San1 and peptide resulted in sim-

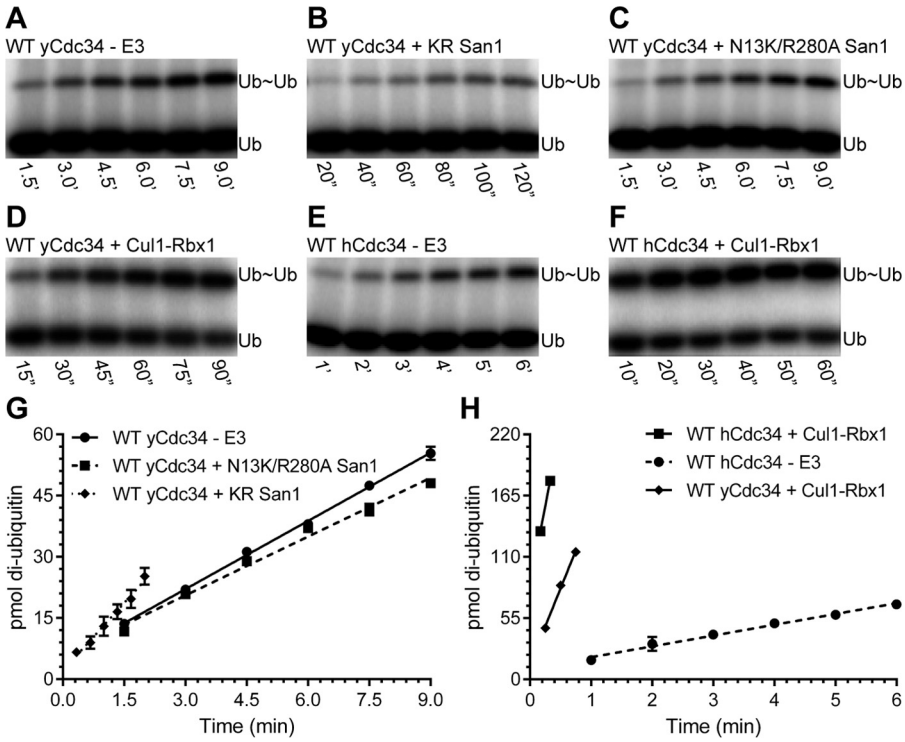

FIGURE 4. **WT Cdc34 activity is only weakly stimulated in the presence of San1.** *A*, diubiquitin synthesis assay for WT Cdc34 (*yCdc34*) showing the time-dependent formation of diubiquitin product. *B*, same as in *A* except KR San1 was added to the reaction mixture before initiation of the reaction by the addition of acceptor ubiquitin. *C*, same as in *B* except with N13K/R280A San1. *D*, same as in *A* except the human SCF Cul1-Rbx1 sub-complex was added to the reaction before acceptor ubiquitin. *E*, same as in *A* except with human WT Cdc34 (*hCdc34*). *F*, same as in *E* except with the addition of Cul1-Rbx1. *G*, quantitation of diubiquitin formation for reactions in *A–C*. Notice that the presence of KR San1 resulted in only modest stimulation of yCdc34 activity. *H*, quantitation of diubiquitin formation for reactions in *D–F*) showing that both yeast and human WT Cdc34 activities were significantly stimulated in the presence of Cul1-Rbx1. Due to the rapid formation of diubiquitin for both hCdc34 and yCdc34 in the presence of Cul1-Rbx1 (and the subsequent deviation of product formation with linearity), notice that only two and three data points, respectively, were used to determine the rates of product formation. *Error bars* represent the S.E. of measurements from duplicate data points.

TABLE 1

Rates of diubiquitin formation for either WT Cdc34 or Ubc1 in the presence or absence of E3s

E2	E3	Rate of Ub Transfer	-Fold change
		pmol min^{-1}	
WT yCdc34		5.6 ± 0.1	
WT yCdc34	N13K/R280A San1	4.8 ± 0.2	1
WT yCdc34	KR San1	11.0 ± 1.1	2
WT yCdc34	Cul1-Rbx1	136.6 ± 6.5	24
WT hCdc34		9.7 ± 0.7	
WT hCdc34	Cul1-Rbx1	283.6 ± 6.7	29
WT Ubc1		0.5 ± 0.04	
WT Ubc1	N13K/R280A San1	1.5 ± 0.05	3
WT Ubc1	KR San1	18.9 ± 1.9	38
WT Ubc1	Cul1-Rbx1	0.7 ± 0.03	1

ilar amounts of substrate conversion to product in comparison to the reaction containing Ubc1 only (Fig. 8*B*). Interestingly, the high molecular weight polyubiquitin chains on substrate were mildly diminished in contrast to the reaction containing only Ubc1 (Fig. 8*A*). These results allow for two major conclusions: 1) ubiquitylation of San1 peptide is more robust in the presence of Ubc1 than with WT Cdc34, and 2) the combination of Ubc1 and Cdc34 in a ubiquitylation reaction does not further enhance product formation when compared with the reaction with Ubc1 alone. Thus, Ubc1 and WT Cdc34 do not function synergistically with San1 *in vitro*, and the presence of Cdc34 may even mildly inhibit the formation of long polyubiquitin chains by Ubc1.

We next compared the kinetics of San1 peptide ubiquitylation with the kinetics of a reaction catalyzed by the SCF ubiquitin ligase as the rates of ubiquitin transfer to SCF-bound substrates are among the fastest in the literature (54). Single-turnover ubiquitylation reactions were assembled with either yeast Cdc34 or Ubc1 and San1 or with SCF in combination with both UbcH5c and human Cdc34 (note that SCF has been shown to function synergistically with these E2s; Ref. 50). Although ~15% of San1 peptide substrate was modified with one or more ubiquitins after 60 s, nearly all of the SCF substrate had been converted to ubiquitylated product within 10 s (Fig. 9). Furthermore, chain elongation on the SCF substrate was far more extensive than on the San1 peptide, hinting that the SCF-catalyzed reaction is also more processive than the San1-catalyzed reaction. In summary, both polyubiquitin chain initiation and extension are far more rapid for SCF-bound substrate than for San1-bound substrate.

Discussion

Using quantitative kinetics and an *in vitro* reconstituted ubiquitylation assay, we demonstrate that the San1 ubiquitin ligase preferentially functions with Ubc1 over Cdc34. First, the affinity of Ubc1 for San1 is much higher in comparison with WT Cdc34. Second, Ubc1 activity is greatly stimulated in the presence of San1, whereas Cdc34 activity is only weakly stimulated by San1. Last, Ubc1 both initiates polyubiquitin chains

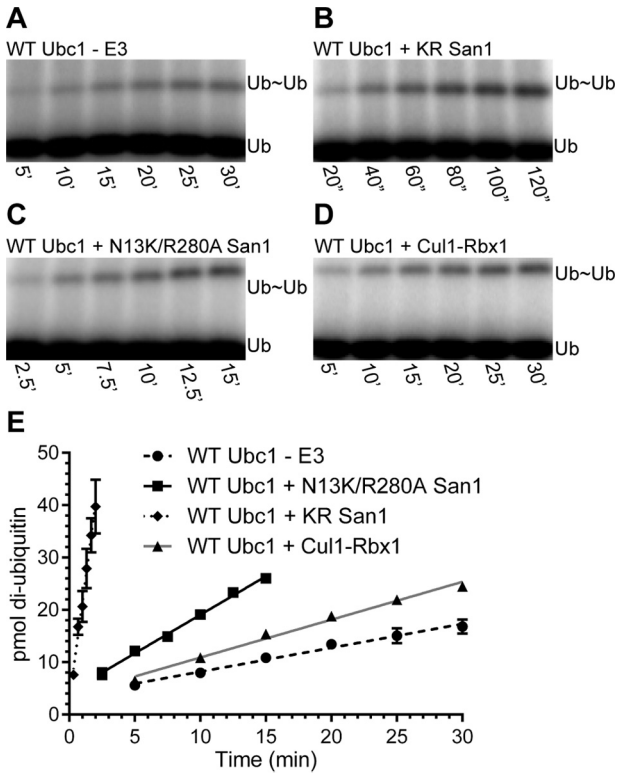

FIGURE 5. **Ubc1 activity is strongly stimulated in the presence of San1.** *A*, diubiquitin synthesis assay for WT Ubc1 showing the time-dependent formation of diubiquitin product. *B*, same as in *A* except KR San1 was added to the reaction mixture before the addition of acceptor ubiquitin. *C*, same as in *B* except with N13K/R280A San1. *D*, same as in *C* except with Cul1-Rbx1. Notice that the presence of KR San1 resulted in the stimulation of Ubc1 activity; however, the addition of Cul1-Rbx1 had no effect on Ubc1 activity. *E*, quantification of diubiquitin formation for reactions in *A–D*. *Error bars* represent the S.E. of measurements from duplicate data points.

and extends them more rapidly on San1-bound substrate than Cdc34.

The greater activity of Ubc1 with San1 in comparison with Cdc34 is surprising given the genetic evidence. For instance, the stability of Sir4-9 protein, a model PQC substrate, was substantially greater in a cdc34-2 temperature-sensitive yeast strain compared with a ubc1Δ strain (29). The discrepancy between the genetic and biochemical results presented here may be caused, at least in part, by the cell cycle arrest phenotype induced by the cdc34-2 allele. On the other hand, conditions in the nucleus, such as E2 protein levels as well as regulation, may affect whether San1 functions preferentially with Cdc34 or Ubc1 in living cells (see below). Regardless, this example highlights how *in vitro* approaches for uncovering mechanistic processes of ubiquitylation can be complementary to *in vivo* approaches.

E2-E3 Interactions during the Ubiquitylation of PQC Substrates; Why High Affinity Binding Is Not Always Warranted—It was noted earlier that the K_m of WT Cdc34 for San1 was ~10-fold higher in comparison with the K_m of WT Cdc34 for the ubiquitin ligase SCF (51). Furthermore, the binding of Cdc34 to San1 is not dependent on the acidic tail domain, which is essential for Cdc34 function with SCF (51). How can these differences be reconciled?

To address this question, it is relevant to examine how the acidic tail promotes Cdc34 binding to SCF. Specifically, the acidic tail drives extremely fast association between Cdc34~ubiquitin and SCF by promoting electrostatic interactions between the acidic tail residues and a basic canyon located near the RING domain on SCF (53). Thus, fast association also enables a rapid rate of Cdc34 dissociation from SCF without compromising high affinity binding. Rapid dynamics between Cdc34 and SCF promotes processive ubiquitin transfer (54), increasing the probability that a substrate-E3 encounter will result in substrate ubiquitylation and degradation.

The rationale for the efficient ubiquitylation of SCF substrates, which include Cdk inhibitors and transcription factors, is that the prompt degradation of these substrates is required for proper signal transduction in the cell. Conversely, the efficient degradation of PQC substrates is likely not beneficial to the cell and may even be harmful. For instance, some proteins may only transiently unfold, and protein chaperones may provide these misfolded proteins with opportunities to regain their native states (55, 56). Thus, the interaction of Cdc34 with San1 in an acidic-tail independent fashion likely serves to decrease the efficiency of polyubiquitin chain formation on San1-bound substrates.

Nevertheless, for Cdc34 and San1 to function together, they must somehow form a complex without involvement of the Cdc34 acidic tail. Interestingly, the K_m of Δ190 Cdc34 for San1 is 2.2 μM, whereas the K_m of Δ190 Cdc34 for SCF has previously been estimated to be 16 μM (51). Thus, San1 circumvents the necessity of the acid tail by having evolved the ability to bind with higher affinity to the Cdc34 catalytic domain. Interestingly, the nuclear concentration of Cdc34 in yeast has been estimated to be ~10 μM (51), high enough to approach saturation of San1 with Cdc34 given the value of K_m (1.7 μM for WT Cdc34). Thus, Cdc34~ubiquitin-San1 complexes can still form in the cell; however, the dynamics of Cdc34 association and dissociation will likely be far slower without participation of the acidic tail, ultimately delaying the subsequent ubiquitylation and degradation of misfolded substrates.

How Multiple E2s Collaborate to Increase the Chances That E3-Substrate Encounters Result in Ubiquitylation; the Hand-off Model—Further evidence that PQC substrate ubiquitylation evolved to be less efficient compared with E3s such as SCF comes from the observation that many E3s including SCF require at least two E2s to function in cells (44–50). In what has been termed the hand-off model, an E2~ubiquitin transfers the first ubiquitin to E3-bound substrate, and chain elongation is accomplished by a different E2 family member. For instance, E2s such as Ubc4 and Ubc5 in yeast (Ube2D1–4 in humans) are very good at transferring a single ubiquitin to a lysine residue on an unmodified protein substrate, but they are not good at building polyubiquitin chains. Conversely, other E2s, such as Cdc34 and Ubc1, are inefficient at transferring the first ubiquitin to substrate but are very good at building polyubiquitin chains.

When E3s such as SCF recruit members from both groups of E2s, the rate of conversion of substrate to poly-ubiquitylated product is increased. By relying only on either Cdc34 or Ubc1 to initiate as well as to extend chains, San1 encounters with misfolded substrate likely results in a lower frequency of substrate poly-ubiquitylation, which may afford them precious time to recover their native folds. Interestingly, it has been shown that

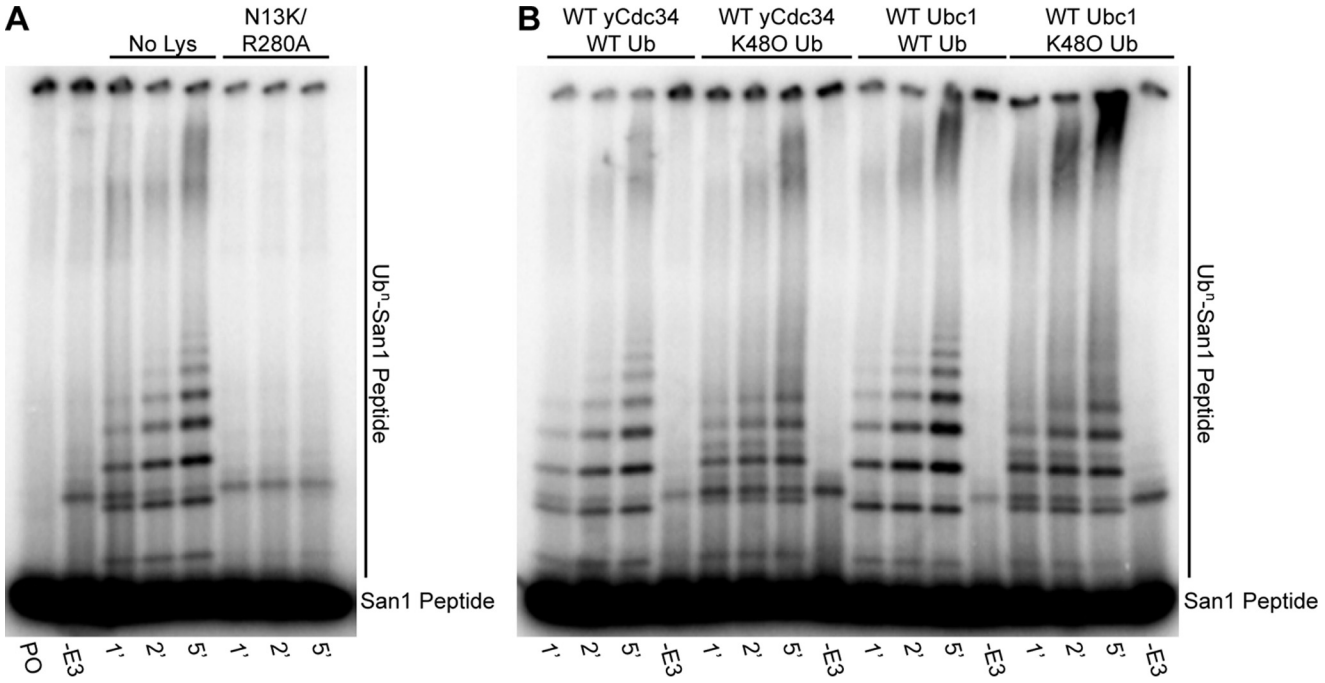

FIGURE 6. **San1 peptide is rapidly ubiquitylated in the presence of KR San1.** *A*, multi-turnover ubiquitylation reactions were carried out in the presence of WT Cdc34 and either KR San1 or N13K/R280A San1. Notice that San1 peptide became ubiquitylated only in the presence of KR San1, indicating that the San1 RING domain and subsequent recruitment of Cdc34~ubiquitin are required for substrate ubiquitylation. *PO* (peptide only) indicates a reaction containing San1 peptide where all additional reaction components were excluded. *B*, multi-turnover ubiquitylation reactions in either the presence of WT Cdc34 or WT Ubc1 and either WT ubiquitin or a Lys-48-only ubiquitin mutant (*K48O*). Notice that product formation is similar in reactions containing WT or K48O ubiquitin, indicating that both WT Cdc34 and Ubc1 likely generate polyubiquitin chains on San1 peptide that are Lys-48-specific.

the order of degradation of substrates of the APC ubiquitin ligase is determined by the efficiency of polyubiquitin chain formation (57). We posit that the lower efficiency of San1-mediated substrate ubiquitylation may function similarly, providing the cell with an additional layer of control regarding the decision event for the degradation of misfolded proteins beyond well established mechanisms such as chaperone-mediated triage (27, 58). On a final note, we acknowledge that our reaction conditions may differ substantially from that in the cell where the localization of the enzymes as well as the presence of additional cofactors may affect the efficiency of ubiquitylation. Future experiments are necessary to address these issues.

Why Does San1 Need 2 E2s That Function Independent of Each Other?—If San1 does not function synergistically with Cdc34 and Ubc1 through a hand-off-based mechanism, why would San1 function with Cdc34 at all, as it prefers Ubc1? First, notice that Cdc34 still assembles polyubiquitin chains containing four or more ubiquitins on a significant fraction of San1 peptides even in the absence of Ubc1 (Fig. 8). Furthermore, it is possible that Ubc1 activity may decrease under certain physiological conditions such as stress or during certain phases of the cell cycle. Because the constant presence of misfolded proteins in the cell requires that PQC processes remain vigilant, San1 must function with an alternate E2 such as Cdc34 if Ubc1 is unavailable. Future work is required to uncover exactly how Ubc1 and Cdc34 coordinate their activities with San1 in the cell. Importantly, the reconstituted *in vitro* ubiquitylation system developed here enables the direct comparison of Ubc1 and Cdc34 activities, providing new insight into how PQC processes may function in the cell.

Experimental Procedures

Cloning—All San1 constructs were amplified by PCR from previously published templates (38). The 5′ primer contained coding sequences for a tobacco etch virus protease cleavage site followed by a protein kinase A (PKA) phosphorylation consensus motif (5′-GGCGGATCCGAGAACCTGTACTTCCAGGGCCGTCGCGGTAGCCTGAGTGAAAGTGGTCAAGAACAAAACA-3′), and the 3′ primer contained a coding sequence for an eight-histidine tag that was appended to the San1 C terminus (5′-GGCCTCGAGTTAATGGTGATGGTGATGGTGATGGTGTTGTGATGATCGTTGCTCATTG-3′). PCR products were digested with the BamHI and Xho1 restriction enzymes followed by ligation into the pGex-4T expression vector. All constructs were verified through DNA sequencing.

Protein Expression and Purification—All recombinant proteins were expressed in *Escherichia coli* using Rosetta 2(DE3)pLysS competent cells (Novagen). Yeast WT and Δ190 Cdc34 were expressed and purified as previously described (51, 54). Yeast Ubc1 was expressed and purified essentially as previously described (46) with the following modifications. Bacterial cells were grown at 37 °C to an optical density of 0.8, after which expression was induced with isopropyl 1-thio-β-D-galactopyranoside for 3 h followed by centrifugation and storage of the cell pellets at −80 °C. Frozen cell pellets were solubilized in a buffer containing 30 mM Tris, pH 7.5, 250 mM NaCl, 20 mM imidazole, 0.1% IgePal, 5% glycerol, and protease inhibitor mixture (PIC, Pierce) followed by sonication. The lysate was cleared by centrifugation and incubated with nickel-nitrilotriacetic acid-agarose beads (Qiagen) and gentle agitation for 1 h at 4 °C.

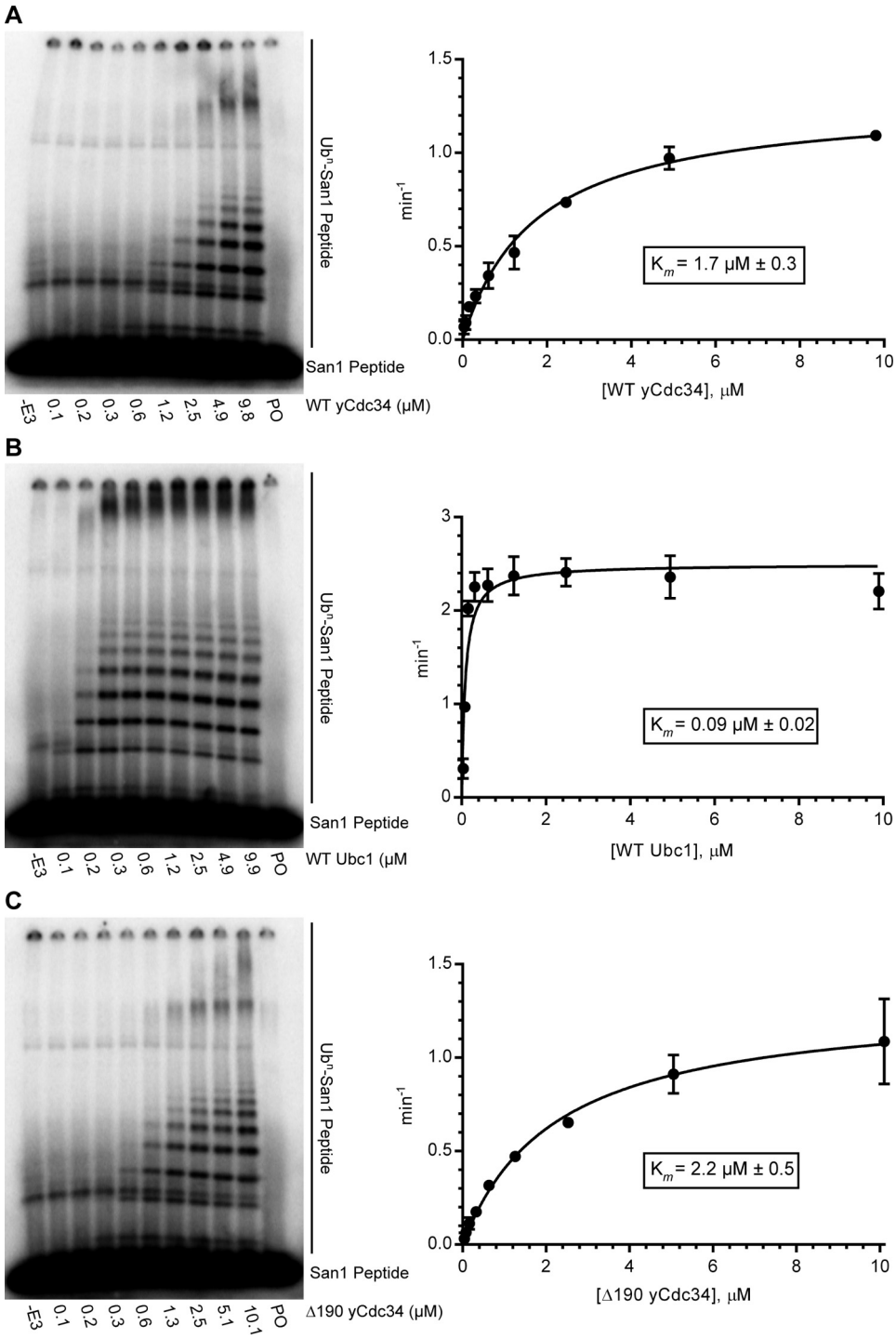

FIGURE 7. **Ubc1 has greater affinity for San1 than Cdc34.** *A*, San1 peptide ubiquitylation reactions containing KR San1 and titrations of WT Cdc34 protein. Each lane represents a single ubiquitylation reaction that was quenched with 2× SDS-PAGE loading buffer after 10 min. *Error bars* represent the S.E. of measurements from duplicate data points. *B*, same as in *A* except with WT Ubc1. Reactions were quenched with SDS-PAGE loading buffer after 6 min. *C*, same as in *A* except with Δ190 Cdc34. Notice that deletion of the Cdc34 acidic tail does not affect the affinity of Cdc34 for San1.

The beads were then repeatedly washed with lysis buffer before the addition of elution buffer (50 mM HEPES, pH 7.5, 200 mM NaCl, and 300 mM imidazole). The eluted protein was concentrated (Amicon Ultra-4, 10,000 nominal molecular weight limit) and loaded onto a Superdex 75 gel filtration column (GE Healthcare) that had been equilibrated in storage buffer (30 mM Tris, pH 8.0, 100 mM NaCl, 1 mM DTT, and 10% glycerol). Fractions containing Ubc1 were collected and concentrated to 170 μM (Fig. 1) before snap-freezing in liquid nitrogen and storage at −80 °C.

E. coli cells for San1 expression were initially grown at 37 °C in LB supplemented with ampicillin (100 μg/ml) and chloramphenicol (25 μg/ml). When the cultures reached an optical density of 0.8, the bacterial cells were then transferred to fresh media lacking antibiotics. Protein expression was induced overnight at 16 °C using isopropyl 1-thio-β-D-galactopyranoside

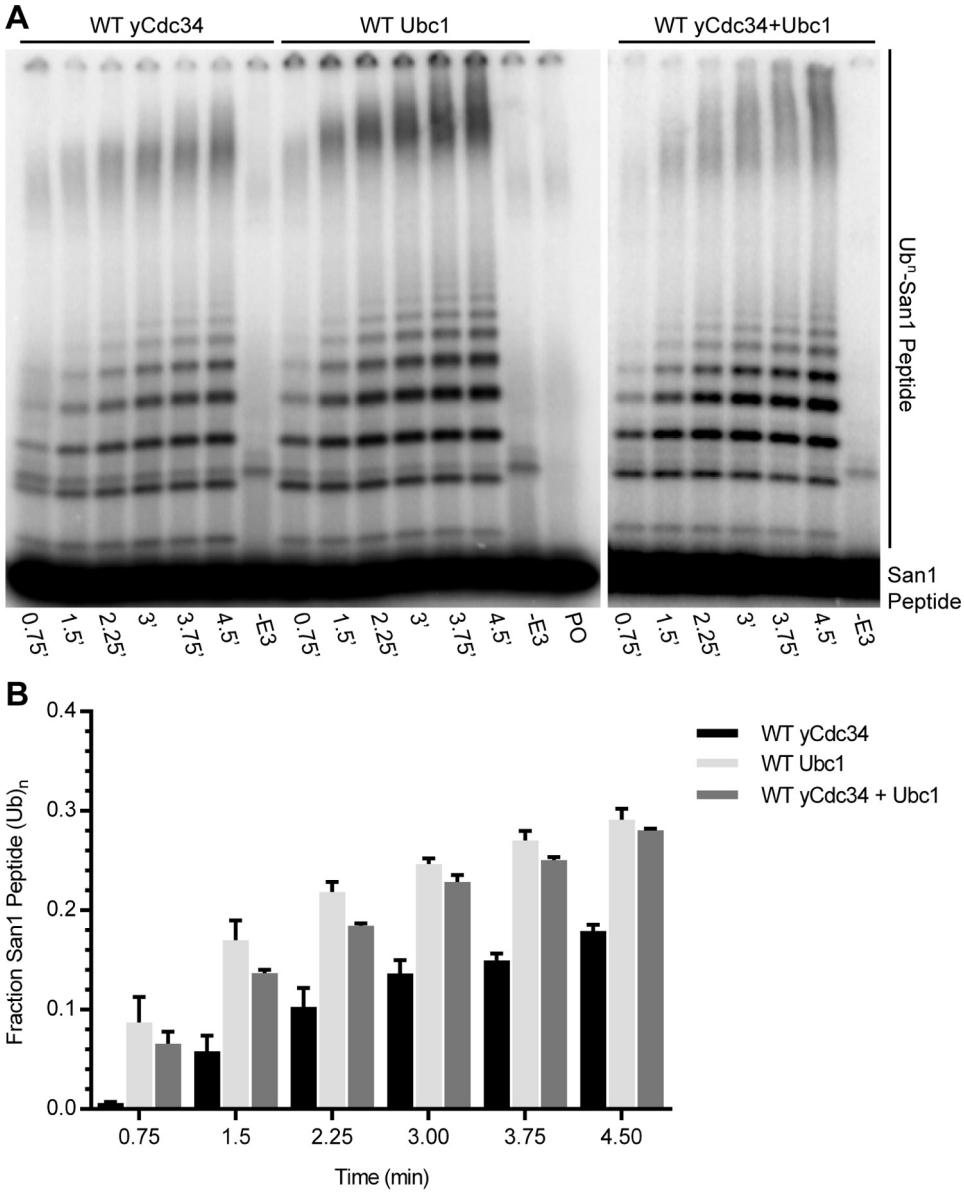

FIGURE 8. **San1 functions preferentially with Ubc1 over WT Cdc34.** *A*, San1 peptide multi-turnover ubiquitylation reactions were carried out in the presence of KR San1 and either WT Ubc1 alone, WT Cdc34 alone, or Ubc1 and WT Cdc34 in combination. Notice that reactions with Ubc1 show intense high molecular weight smears corresponding to long polyubiquitin chains on substrate in comparison with the reaction containing WT Cdc34 alone. *B*, quantification of the conversion of San1 peptide substrate into products containing one or more ubiquitins. Notice that substrate is converted to product more rapidly in the presence of Ubc1 than with WT Cdc34, and the reaction with both Ubc1 and WT Cdc34 does not further enhance product formation in comparison with Ubc1 alone. *Error bars* represent the S.E. of measurement derived from duplicate data points.

(0.4 mM). Bacterial cell pellets were solubilized in lysis buffer (30 mM Tris, pH 7.5, 200 mM NaCl, 5 mM DTT, 1 mM EDTA, 10% glycerol, and protease inhibitor mixture) and disrupted by sonication. Lysates were prepared by centrifugation and then incubated with glutathione-Sepharose 4B beads (GE Healthcare) for 3 h at 4 °C. Beads were then collected and washed repeatedly with lysis buffer lacking protease inhibitor mixture and EDTA. Recombinant GST-San1 protein was eluted in a buffer containing 50 mM Tris, pH 8.0, 200 mM NaCl, and 40 mM glutathione. These proteins were then incubated with tobacco etch virus protease overnight at 4 °C followed by loading onto a 1-ml HisTrap HP column (GE Healthcare) that had been equilibrated in buffer A (50 mM HEPES, pH 7.5, 200 mM NaCl, 20 mM imidazole, 5% glycerol). Histidine-tagged San1 proteins were eluted from the column using a linear gradient of buffer B (50 mM HEPES, pH 7.5, 200 mM NaCl, 300 mM imidazole, and 5% glycerol). Fractions containing San1 were dialyzed into storage buffer by repeatedly diluting the protein sample in storage buffer followed by concentration (Amicon Ultra-4 10,000 nominal molecular weight limit). Purified San1 proteins (Fig. 1) were concentrated to ~20 μM and flash-frozen in liquid nitrogen before storage at −80 °C.

In Vitro San1 Autoubiquitylation Assay—San1 autoubiquitylation assays were performed in a reaction buffer containing 30 mM Tris, pH 7.5, 5 mM $MgCl_2$, 2 mM ATP, and 2 mM DTT. San1 proteins (8 μM) were radiolabeled in the presence of γ-^{32}P-labeled ATP (PerkinElmer Life Sciences) and cAMP-dependent protein kinase (New England BioLabs) for 1 h at 30 °C. WT

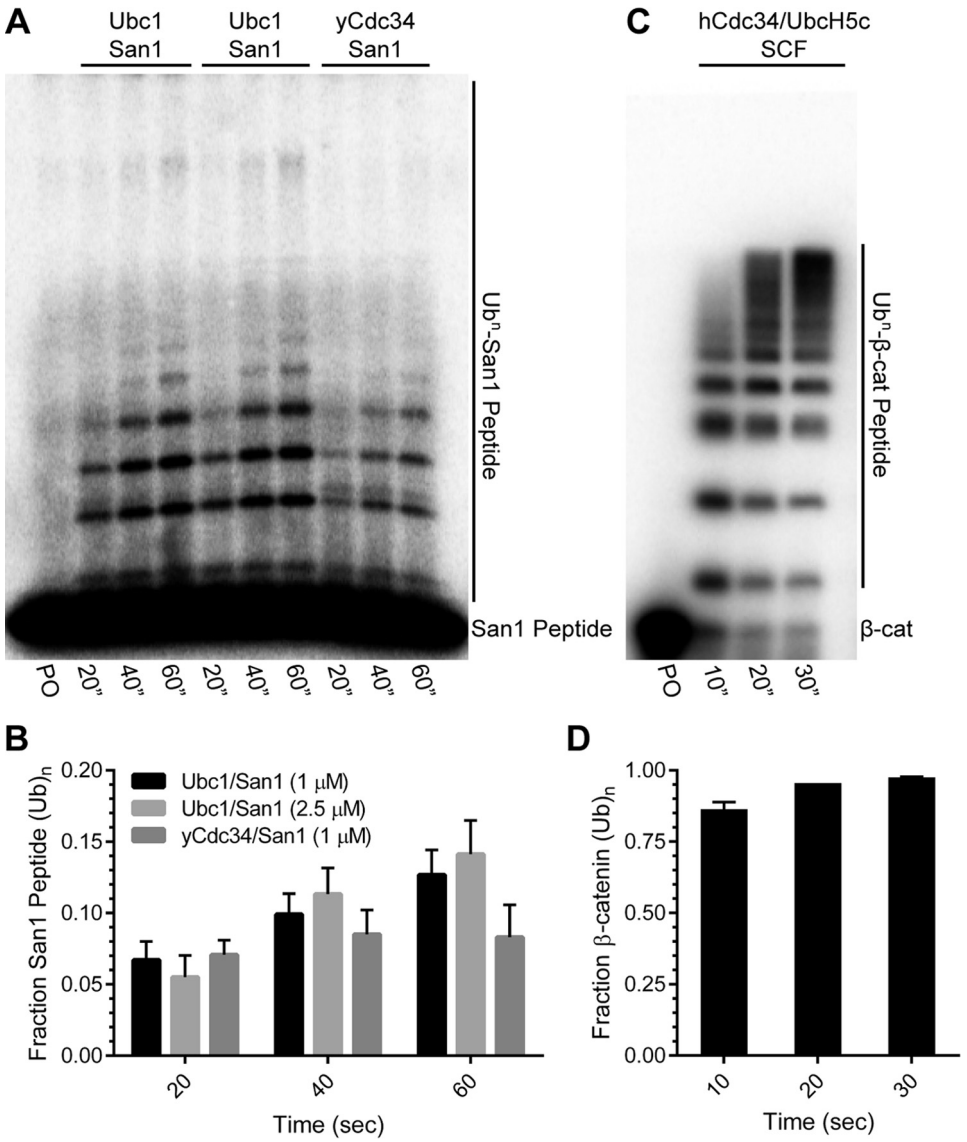

FIGURE 9. **Single-turnover reactions demonstrate that SCF-bound substrate is far more rapidly converted into ubiquitylated product than San1-bound substrate.** *A*, single-turnover ubiquitylation reactions were carried out in the presence of either WT Ubc1 and KR San1 (1 μM, *lanes 2–4*; 2.5 μM, *lanes 5–7*) or WT Cdc34 and KR San1 (*lanes 8–10*). Notice that San1 peptide ubiquitylation is similar in reactions containing either 1 μM or 2.5 μM KR San1, suggesting that 1 μM San1 is sufficient to saturate San1 peptide. *PO* (peptide only) indicates a reaction containing San1 peptide where all additional reaction components were excluded. *B*, quantification of the conversion of San1 peptide substrate into products containing one or more ubiquitins. *Error bars* represent the S.E. of measurement derived from duplicate data points. *C*, single-turnover ubiquitylation reactions were carried out in the presence of WT UbcH5c and WT human Cdc34 (hCdc34) and neddylated SCF. Notice that nearly all β-catenin peptide substrate (β-*cat*) is converted into ubiquitylated product by 10 s. *D*, quantification of the conversion of β-catenin substrate into products containing one or more ubiquitins. *Error bars* represent the S.E. of measurement derived from duplicate data points.

ubiquitin (60 μM), human E1 (1 μM; note that San1 activity was indistinguishable in the presence of either human or yeast E1), and either Cdc34 or Ubc1 (10 μM) were first incubated for 1 min at room temperature followed by the addition of San1 (1 μM). Time points were quenched in SDS-PAGE loading buffer, and San1 substrate and ubiquitylated products were resolved on 7.5% SDS-PAGE gels (Lonza). Gels were then dried and exposed to a phosphor screen before imaging on a Typhoon 9410. The quantification of substrate and product levels was performed using ImageQuant software (GE Healthcare). The fraction of ubiquitin-modified San1 was calculated as the ratio of San1 products that had been modified by one or more ubiquitins and the total signal in the lane. Background corrections were performed using a ubiquitylation reaction that contained all components except ubiquitin. The rate of product formation in Fig. 2 was determined by performing linear regression (GraphPad Prism, Version 6.07). The initial rate of product formation in Fig. 3 was determined by fitting the data to a one-phase association model by nonlinear regression. The initial velocity was then estimated by determining the slope of the linear phase of the curve.

E2 Activation Assay—The stimulation of E2 activity by San1 was followed using a previously described diubiquitin synthesis assay (51). E2 activation assays were performed in the same reaction buffer as above. Human E1 (1 μM), ^{32}P-labeled K48R donor ubiquitin (10 μM), and either Cdc34 or Ubc1 (10 μM) were briefly incubated followed by either the addition of San1 protein, where all lysine residues had been mutated to arginine

(KR San1; 1 μM), or buffer and incubation for 2 min. Acceptor ubiquitin that contained an aspartic acid residue at its C terminus (50 μM) was then introduced to initiate diubiquitin synthesis. Time points were quenched in non-reducing SDS-PAGE loading buffer. Reaction substrates and products were resolved on 4–20% SDS-PAGE gels (Lonza). The amounts of substrates and products were quantified using ImageQuant (GE Healthcare). The amount of diubiquitin (pmol) was plotted as a function of time, and the rates of product formation were determined by linear regression.

San1 Peptide Multi-turnover Ubiquitylation Reactions—The San1 peptide (acetyl-CGSRRGSYNASSGEQMLSRTGFFLV-LIVGQLHNPVK; New England Peptide) was radiolabeled (50 μM) in the presence of γ-^{32}P-labeled ATP (PerkinElmer Life Sciences) and cAMP-dependent protein kinase (New England Biolabs) for 1 h at 30 °C in a reaction buffer that had been supplemented with Tween 20 (0.1%). All multi-turnover reactions were carried out in a reaction buffer containing 30 mM Tris, pH 7.5, 5 mm $MgCl_2$, 2 mM ATP, 2 mM DTT, and 0.1% Tween 20. Human E1 (1 μM), WT or Lys-48-only ubiquitin (60 μM; Boston Biochem), E2 (10 μM), and KR San1 (0.5 μM) were incubated for 2 min. San1 peptide (5 μM) was then added to initiate the reaction. Time points were quenched in SDS-PAGE buffer, and ubiquitylated products were separated on 4–20% SDS-PAGE gels (Lonza). Gels were processed, and the fraction of ubiquitylated San1 peptide was calculated by dividing the amount of peptide that had been modified by one or more ubiquitins by the total signal in the lane.

Determining the K_m of Cdc34 or Ubc1 for San1—Experiments to estimate the K_m of Cdc34 or Ubc1 for San1 were performed in a reaction buffer containing 30 mM Tris, pH 7.5, 5 mm $MgCl_2$, 2 mM ATP, 2 mM DTT, and 0.1% Tween 20. A master mix containing ubiquitin (60 μM) and human E1 (1 μM) in reaction buffer was assembled and distributed to individual tubes. Next, a 2-fold dilution series was established for either yCdc34 (WT and Δ190) or Ubc1. Aliquots of either Cdc34 or Ubc1 at each concentration were then added to each tube containing E1 and ubiquitin and incubated for 1 min. KR San1 (0.1 μM) was then added to each tube and incubated for an additional 2 min. Radiolabeled San1 peptide (5 μM) was added to initiate the reaction. Reactions were quenched with 2× SDS-PAGE loading buffer at 6 min (Ubc1) or 10 min (yCdc34) to maintain ~20–30% product conversion and ensure linearity of the reaction velocities at the highest concentrations of Ubc1 or yCdc34. Substrates and products were resolved on a 4–20% SDS-PAGE gel, dried, and exposed to a phosphor screen. Quantification of substrate and product was performed as described above. The rate of San1 peptide ubiquitylation was calculated by dividing the fraction of ubiquitylated product by the time of incubation and multiplying by the ratio of the concentrations of peptide and KR San1. These data were then fit to the Michaelis-Menten equation by nonlinear regression.

Single-turnover Reactions—San1 single-turnover reactions were carried out in a reaction buffer containing 30 mM Tris, pH 7.5, 5 mm $MgCl_2$, 2 mM ATP, 2 mM DTT, and 0.1% Tween 20. Human E1 (1 μM), wild type ubiquitin (60 μM), E2 (10 μM), and KR San1 (2.5 μM or 1 μM) were mixed together and incubated for 2 min. Radiolabeled San1 peptide (0.5 μM) was added to initiate the reaction. Reactions were quenched in SDS-PAGE buffer at the indicated time points, and products were separated on 4–20% SDS-PAGE gel. Gels were dried, exposed, imaged, and quantified as described for the multi-turnover reactions.

Previously described SCF single-turnover reactions (59) were carried out in reaction buffer containing 30 mM Tris, pH 7.5, 100 mM NaCl, 5 mM $MgCl_2$, 2 mM ATP, and 2 mM DTT. Human E1 (1 μM), wild type ubiquitin (60 μM), and both UbcH5c and human Cdc34 (10 μM each) were mixed together and incubated for 1 min. Equimolar concentrations of neddylated Cul1-Rbx1 and βTrcp-Skp1 complexes (59) (1 μM) were added and incubated for 1 min. Radiolabeled β-catenin peptide substrate (0.25 μM) was added to initiate the reaction. Reactions were quenched in 2× SDS-PAGE loading buffer at the indicated time points, and substrates and products were separated on a 18% SDS-PAGE gel. Gels were dried, exposed, imaged, and quantified as described as above.

Author Contributions—R. I. conducted most of the experiments, analyzed the results, and helped with experimental design. D. S. conducted some of the experiments in Figs. 4 and 9 and helped with experimental design. E. K. F. and R. G. G. had substantial contributions to experimental conception and design. G. K. conceived the idea for the project, helped with experimental design, and wrote the manuscript with contributions from all other authors.

Acknowledgments—We thank Drs. Thibault Mayor and Ray Deshaies for thoughtful comments during the preparation of the manuscript and Casey Hall of the UNLV Genomics Core Facility for DNA sequencing. G. K. thanks Kenny Barker for inspiration.

References

1. Kleiger, G., and Mayor, T. (2014) Perilous journey: a tour of the ubiquitin-proteasome system. *Trends Cell Biol.* **24,** 352–359
2. Deshaies, R. J., and Joazeiro, C. A. (2009) RING domain E3 ubiquitin ligases. *Annu. Rev. Biochem.* **78,** 399–434
3. Komander, D., and Rape, M. (2012) The ubiquitin code. *Annu. Rev. Biochem.* **81,** 203–229
4. Schulman, B. A., and Harper, J. W. (2009) Ubiquitin-like protein activation by E1 enzymes: the apex for downstream signalling pathways. *Nat. Rev. Mol. Cell Biol.* **10,** 319–331
5. Ye, Y., and Rape, M. (2009) Building ubiquitin chains: E2 enzymes at work. *Nat. Rev. Mol. Cell Biol.* **10,** 755–764
6. Branigan, E., Plechanovová, A., Jaffray, E. G., Naismith, J. H., and Hay, R. T. (2015) Structural basis for the RING-catalyzed synthesis of K63-linked ubiquitin chains. *Nat. Struct. Mol. Biol.* **22,** 597–602
7. Das, R., Liang, Y. H., Mariano, J., Li, J., Huang, T., King, A., Tarasov, S. G., Weissman, A. M., Ji, X., and Byrd, R. A. (2013) Allosteric regulation of E2:E3 interactions promote a processive ubiquitination machine. *EMBO J.* **32,** 2504–2516
8. Dou, H., Buetow, L., Sibbet, G. J., Cameron, K., and Huang, D. T. (2012) BIRC7-E2 ubiquitin conjugate structure reveals the mechanism of ubiquitin transfer by a RING dimer. *Nat. Struct. Mol. Biol.* **19,** 876–883
9. Plechanovová, A., Jaffray, E. G., Tatham, M. H., Naismith, J. H., and Hay, R. T. (2012) Structure of a RING E3 ligase and ubiquitin-loaded E2 primed for catalysis. *Nature* **489,** 115–120
10. Pruneda, J. N., Littlefield, P. J., Soss, S. E., Nordquist, K. A., Chazin, W. J., Brzovic, P. S., and Klevit, R. E. (2012) Structure of an E3:E2~Ub complex reveals an allosteric mechanism shared among RING/U-box ligases. *Mol. Cell* **47,** 933–942
11. Scott, D. C., Sviderskiy, V. O., Monda, J. K., Lydeard, J. R., Cho, S. E.,

Harper, J. W., and Schulman, B. A. (2014) Structure of a RING E3 trapped in action reveals ligation mechanism for the ubiquitin-like protein NEDD8. *Cell* **157,** 1671–1684
12. Piotrowski, J., Beal, R., Hoffman, L., Wilkinson, K. D., Cohen, R. E., and Pickart, C. M. (1997) Inhibition of the 26 S proteasome by polyubiquitin chains synthesized to have defined lengths. *J. Biol. Chem.* **272,** 23712–23721
13. Thrower, J. S., Hoffman, L., Rechsteiner, M., and Pickart, C. M. (2000) Recognition of the polyubiquitin proteolytic signal. *EMBO J.* **19,** 94–102
14. Lu, Y., Lee, B. H., King, R. W., Finley, D., and Kirschner, M. W. (2015) Substrate degradation by the proteasome: a single-molecule kinetic analysis. *Science* **348,** 1250834
15. Shabek, N., Herman-Bachinsky, Y., Buchsbaum, S., Lewinson, O., Haj-Yahya, M., Hejjaoui, M., Lashuel, H. A., Sommer, T., Brik, A., and Ciechanover, A. (2012) The size of the proteasomal substrate determines whether its degradation will be mediated by mono- or polyubiquitylation. *Mol. Cell* **48,** 87–97
16. Chen, B., Retzlaff, M., Roos, T., and Frydman, J. (2011) Cellular strategies of protein quality control. *Cold Spring Harb. Perspect. Biol.* **3,** a004374
17. Bengtson, M. H., and Joazeiro, C. A. (2010) Role of a ribosome-associated E3 ubiquitin ligase in protein quality control. *Nature* **467,** 470–473
18. Brandman, O., and Hegde, R. S. (2016) Ribosome-associated protein quality control. *Nat. Struct. Mol. Biol.* **23,** 7–15
19. Verma, R., Oania, R. S., Kolawa, N. J., and Deshaies, R. J. (2013) Cdc48/p97 promotes degradation of aberrant nascent polypeptides bound to the ribosome. *eLife* **2,** e00308
20. Wang, F., Durfee, L. A., and Huibregtse, J. M. (2013) A cotranslational ubiquitination pathway for quality control of misfolded proteins. *Mol. Cell* **50,** 368–378
21. Eisele, F., and Wolf, D. H. (2008) Degradation of misfolded protein in the cytoplasm is mediated by the ubiquitin ligase Ubr1. *FEBS Lett.* **582,** 4143–4146
22. Fang, N. N., Chan, G. T., Zhu, M., Comyn, S. A., Persaud, A., Deshaies, R. J., Rotin, D., Gsponer, J., and Mayor, T. (2014) Rsp5/Nedd4 is the main ubiquitin ligase that targets cytosolic misfolded proteins following heat stress. *Nat. Cell Biol.* **16,** 1227–1237
23. Fang, N. N., Ng, A. H., Measday, V., and Mayor, T. (2011) Hul5 HECT ubiquitin ligase plays a major role in the ubiquitylation and turnover of cytosolic misfolded proteins. *Nat. Cell Biol.* **13,** 1344–1352
24. Heck, J. W., Cheung, S. K., and Hampton, R. Y. (2010) Cytoplasmic protein quality control degradation mediated by parallel actions of the E3 ubiquitin ligases Ubr1 and San1. *Proc. Natl. Acad. Sci. U.S.A.* **107,** 1106–1111
25. Murata, S., Minami, Y., Minami, M., Chiba, T., and Tanaka, K. (2001) CHIP is a chaperone-dependent E3 ligase that ubiquitylates unfolded protein. *EMBO Rep* **2,** 1133–1138
26. Christianson, J. C., and Ye, Y. (2014) Cleaning up in the endoplasmic reticulum: ubiquitin in charge. *Nat. Struct. Mol. Biol.* **21,** 325–335
27. Buchberger, A., Bukau, B., and Sommer, T. (2010) Protein quality control in the cytosol and the endoplasmic reticulum: brothers in arms. *Mol. Cell* **40,** 238–252
28. Baker, M. J., Tatsuta, T., and Langer, T. (2011) Quality control of mitochondrial proteostasis. *Cold Spring Harb. Perspect. Biol.* **3,** a007559
29. Gardner, R. G., Nelson, Z. W., and Gottschling, D. E. (2005) Degradation-mediated protein quality control in the nucleus. *Cell* **120,** 803–815
30. Aguzzi, A., and O'Connor, T. (2010) Protein aggregation diseases: pathogenicity and therapeutic perspectives. *Nat. Rev. Drug Discov.* **9,** 237–248
31. Tramutola, A., Di Domenico, F., Barone, E., Perluigi, M., and Butterfield, D. A. (2016) It is all about (u)biquitin: role of altered ubiquitin-proteasome system and UCHL1 in Alzheimer disease. *Oxid. Med. Cell Longev.* **2016,** 2756068
32. Heo, J. M., Ordureau, A., Paulo, J. A., Rinehart, J., and Harper, J. W. (2015) The PINK1-PARKIN mitochondrial ubiquitylation pathway drives a program of OPTN/NDP52 recruitment and TBK1 activation to promote mitophagy. *Mol. Cell* **60,** 7–20
33. Lee, J. Y., Nagano, Y., Taylor, J. P., Lim, K. L., and Yao, T. P. (2010) Disease-causing mutations in parkin impair mitochondrial ubiquitination, aggregation, and HDAC6-dependent mitophagy. *J. Cell Biol.* **189,** 671–679
34. Sarraf, S. A., Raman, M., Guarani-Pereira, V., Sowa, M. E., Huttlin, E. L., Gygi, S. P., and Harper, J. W. (2013) Landscape of the PARKIN-dependent ubiquitylome in response to mitochondrial depolarization. *Nature* **496,** 372–376
35. Woulfe, J. (2008) Nuclear bodies in neurodegenerative disease. *Biochim. Biophys. Acta* **1783,** 2195–2206
36. Amm, I., Sommer, T., and Wolf, D. H. (2014) Protein quality control and elimination of protein waste: the role of the ubiquitin-proteasome system. *Biochim. Biophys. Acta* **1843,** 182–196
37. Dasgupta, A., Ramsey, K. L., Smith, J. S., and Auble, D. T. (2004) Sir Antagonist 1 (San1) is a ubiquitin ligase. *J. Biol. Chem.* **279,** 26830–26838
38. Fredrickson, E. K., Clowes Candadai, S. V., Tam, C. H., and Gardner, R. G. (2013) Means of self-preservation: how an intrinsically disordered ubiquitin-protein ligase averts self-destruction. *Mol. Biol. Cell* **24,** 1041–1052
39. Fredrickson, E. K., Gallagher, P. S., Clowes Candadai, S. V., and Gardner, R. G. (2013) Substrate recognition in nuclear protein quality control degradation is governed by exposed hydrophobicity that correlates with aggregation and insolubility. *J. Biol. Chem.* **288,** 6130–6139
40. Fredrickson, E. K., Rosenbaum, J. C., Locke, M. N., Milac, T. I., and Gardner, R. G. (2011) Exposed hydrophobicity is a key determinant of nuclear quality control degradation. *Mol. Biol. Cell* **22,** 2384–2395
41. Gallagher, P. S., Clowes Candadai, S. V., and Gardner, R. G. (2014) The requirement for Cdc48/p97 in nuclear protein quality control degradation depends on the substrate and correlates with substrate insolubility. *J. Cell Sci.* **127,** 1980–1991
42. Rosenbaum, J. C., Fredrickson, E. K., Oeser, M. L., Garrett-Engele, C. M., Locke, M. N., Richardson, L. A., Nelson, Z. W., Hetrick, E. D., Milac, T. I., Gottschling, D. E., and Gardner, R. G. (2011) Disorder targets misorder in nuclear quality control degradation: a disordered ubiquitin ligase directly recognizes its misfolded substrates. *Mol. Cell* **41,** 93–106
43. Rosenbaum, J. C., and Gardner, R. G. (2011) How a disordered ubiquitin ligase maintains order in nuclear protein homeostasis. *Nucleus* **2,** 264–270
44. Christensen, D. E., Brzovic, P. S., and Klevit, R. E. (2007) E2-BRCA1 RING interactions dictate synthesis of mono- or specific polyubiquitin chain linkages. *Nat. Struct. Mol. Biol.* **14,** 941–948
45. Kim, J. H., Choi, J. S., Kim, S., Kim, K., Myung, P. K., Park, S. G., Seo, Y. S., and Park, B. C. (2015) Synergistic effect of two E2 ubiquitin conjugating enzymes in SCF(hFBH1) catalyzed polyubiquitination. *BMB Rep.* **48,** 25–29
46. Rodrigo-Brenni, M. C., and Morgan, D. O. (2007) Sequential E2s drive polyubiquitin chain assembly on APC targets. *Cell* **130,** 127–139
47. Wickliffe, K. E., Lorenz, S., Wemmer, D. E., Kuriyan, J., and Rape, M. (2011) The mechanism of linkage-specific ubiquitin chain elongation by a single-subunit E2. *Cell* **144,** 769–781
48. Wickliffe, K. E., Williamson, A., Meyer, H. J., Kelly, A., and Rape, M. (2011) K11-linked ubiquitin chains as novel regulators of cell division. *Trends Cell Biol.* **21,** 656–663
49. Williamson, A., Wickliffe, K. E., Mellone, B. G., Song, L., Karpen, G. H., and Rape, M. (2009) Identification of a physiological E2 module for the human anaphase-promoting complex. *Proc. Natl. Acad. Sci. U.S.A.* **106,** 18213–18218
50. Wu, K., Kovacev, J., and Pan, Z. Q. (2010) Priming and extending: a UbcH5/Cdc34 E2 handoff mechanism for polyubiquitination on a SCF substrate. *Mol. Cell* **37,** 784–796
51. Kleiger, G., Hao, B., Mohl, D. A., and Deshaies, R. J. (2009) The acidic tail of the Cdc34 ubiquitin-conjugating enzyme functions in both binding to and catalysis with ubiquitin ligase SCFCdc4. *J. Biol. Chem.* **284,** 36012–36023
52. Petroski, M. D., and Deshaies, R. J. (2005) Mechanism of lysine 48-linked ubiquitin-chain synthesis by the cullin-RING ubiquitin-ligase complex SCF-Cdc34. *Cell* **123,** 1107–1120
53. Kleiger, G., Saha, A., Lewis, S., Kuhlman, B., and Deshaies, R. J. (2009) Rapid E2-E3 assembly and disassembly enable processive ubiquitylation of cullin-RING ubiquitin ligase substrates. *Cell* **139,** 957–968
54. Pierce, N. W., Kleiger, G., Shan, S. O., and Deshaies, R. J. (2009) Detection of sequential polyubiquitylation on a millisecond timescale. *Nature* **462,** 615–619

55. Hipp, M. S., Park, S. H., and Hartl, F. U. (2014) Proteostasis impairment in protein-misfolding and -aggregation diseases. *Trends Cell Biol.* **24,** 506–514
56. Kim, Y. E., Hipp, M. S., Bracher, A., Hayer-Hartl, M., and Hartl, F. U. (2013) Molecular chaperone functions in protein folding and proteostasis. *Annu. Rev. Biochem.* **82,** 323–355
57. Rape, M., Reddy, S. K., and Kirschner, M. W. (2006) The processivity of multiubiquitination by the APC determines the order of substrate degradation. *Cell* **124,** 89–103
58. Benyair, R., Ron, E., and Lederkremer, G. Z. (2011) Protein quality control, retention, and degradation at the endoplasmic reticulum. *Int. Rev. Cell Mol. Biol.* **292,** 197–280
59. Saha, A., and Deshaies, R. J. (2008) Multimodal activation of the ubiquitin ligase SCF by Nedd8 conjugation. *Mol. Cell* **32,** 21–31